ARTICLE

Prediction of angle closure after laser peripheral iridotomy: The fourteen-year Zhongshan Angle Closure Prevention trial

Yixiong Yuan,[1,2,3,9] Shaopeng Yang,[1,2,3,9] Wei Wang,[1,2,3,4,*] Benjamin Y. Xu,[5] Cong Li,[1,2,3] Ruilin Xiong,[1,2,3] Chimei Liao,[1,2,3] Jian Zhang,[1,2,3] Qiuxia Yin,[1,2,3] Yingfeng Zheng,[1,2,3] David S. Friedman,[6] Paul J. Foster,[7] and Mingguang He[1,8]

*Correspondence: wangwei@gzzoc.com

Received: July 20, 2023; Accepted: November 6, 2023; Published Online: November 15, 2023; https://doi.org/10.59717/j.xinn-med.2023.100033

GRAPHICAL ABSTRACT

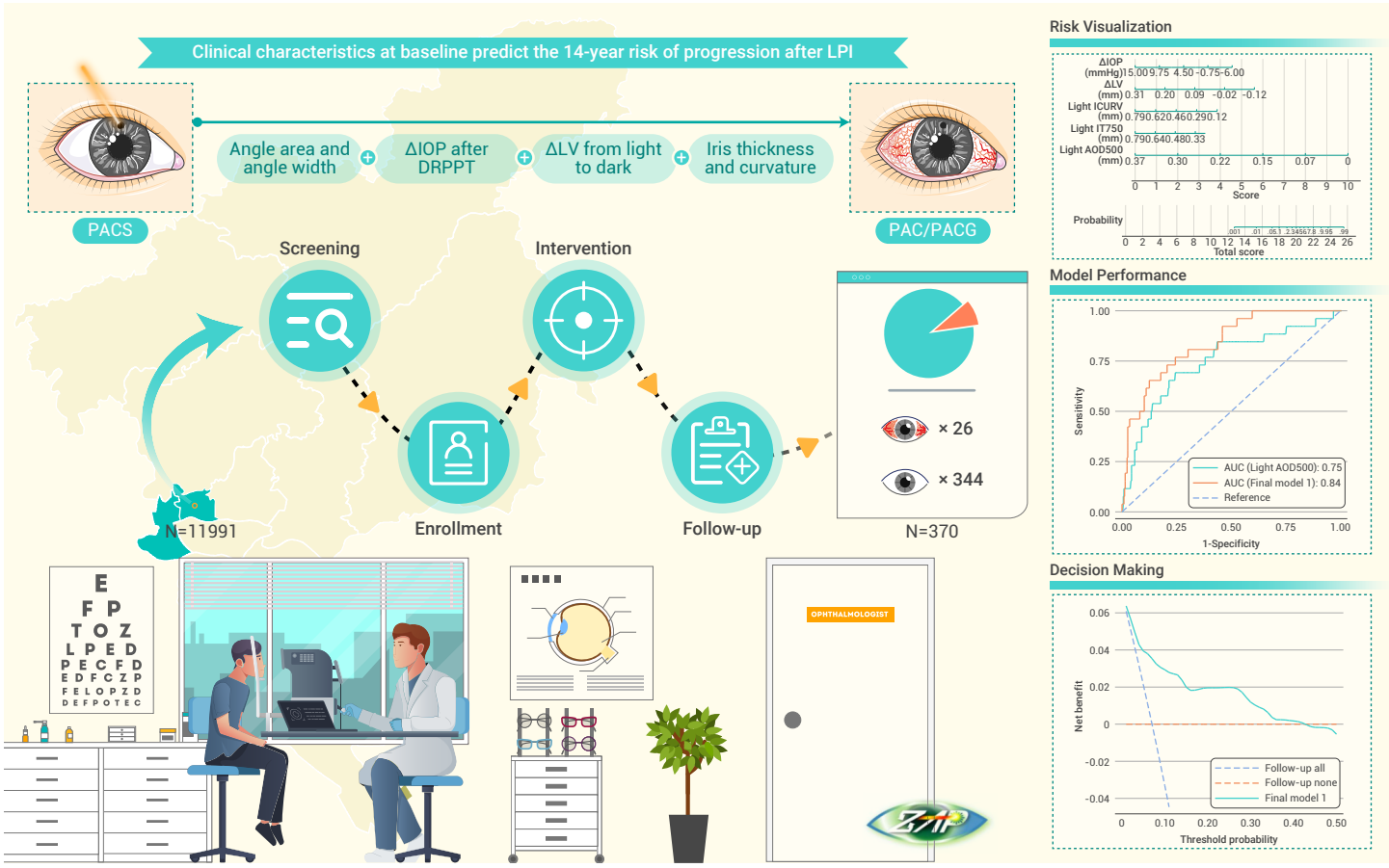

PUBLIC SUMMARY

- Anterior chamber angle can continue to narrow after laser peripheral iridotomy.
- Long-term risk of progression after laser peripheral iridotomy can be predicted.
- The narrowing of anterior chamber angle is an important risk factor.
- Dynamic changes of intraocular pressure and lens vault are additional predictors.

ARTICLE

www.the-innovation.org/medicine

Prediction of angle closure after laser peripheral iridotomy: The fourteen-year Zhongshan Angle Closure Prevention trial

Yixiong Yuan,[1,2,3,9] Shaopeng Yang,[1,2,3,9] Wei Wang,[1,2,3,4,*] Benjamin Y. Xu,[5] Cong Li,[1,2,3] Ruilin Xiong,[1,2,3] Chimei Liao,[1,2,3] Jian Zhang,[1,2,3] Qiuxia Yin,[1,2,3] Yingfeng Zheng,[1,2,3] David S. Friedman,[6] Paul J. Foster,[7] and Mingguang He[1,8]

[1]State Key Laboratory of Ophthalmology, Zhongshan Ophthalmic Center, Sun Yat-sen University, Guangzhou 510060, China
[2]Guangdong Provincial Key Laboratory of Ophthalmology and Visual Science, Guangzhou 510060, China
[3]Guangdong Provincial Clinical Research Center for Ocular Diseases, Guangzhou 510060, China
[4]Hainan Eye Hospital and Key Laboratory of Ophthalmology, Zhongshan Ophthalmic Center, Sun Yat-sen University, Haikou 570311, China
[5]Roski Eye Institute, Keck School of Medicine, University of Southern California, Los Angeles, CA 90033, USA
[6]Department of Ophthalmology, Massachusetts Eye and Ear, Harvard Medical School, Harvard Medical School, Boston, MA 02114, USA
[7]NIHR Biomedical Research Centre at Moorfields Eye Hospital and UCL Institute of Ophthalmology, London, EC1V 2PD, UK
[8]Experimental Ophthalmology, The Hong Kong Polytechnic University, Hong Kong 999077, China
[9]These authors contributed equally
*Correspondence: wangwei@gzzoc.com

Received: July 20, 2023; Accepted: November 6, 2023; Published Online: November 15, 2023; https://doi.org/10.59717/j.xinn-med.2023.100033

Citation: Yuan Y., Yang S., Wang W., et al., (2023). Prediction of angle closure after laser peripheral iridotomy: The fourteen-year Zhongshan Angle Closure Prevention trial. The Innovation Medicine **1(3)**, 100033.

Anterior chamber angles in primary angle closure suspects (PACS) can continue to narrow after laser peripheral iridotomy (LPI). The aim of this study is to identify risk factors and develop prediction models for the progression in LPI-treated eyes during a 14-year follow-up. From 2008 to 2010, 889 Chinese participants aged 50-70 years with bilateral PACS were enrolled in the Zhongshan Angle Closure Prevention (ZAP) trial and received LPI in one randomly selected eye. Examinations before LPI included Goldmann tonometry, ultrasound A-scan biometry, both light-room and dark-room anterior-segment optical coherence tomography (AS-OCT). Logistic regression models were built to predict the 14-year risk of progression in PACS eyes after LPI (peripheral anterior synechiae, intraocular pressure [IOP] > 24 mmHg, or acute angle closure). Within 370 eligible PACS eyes, 26 progressed to PAC during 14 years after LPI. For both light-room and dark-room AS-OCT metrics before LPI, the narrowing of anterior chamber angle was identified as risk factor for the 14-year risk of progression in LPI-treated PACS eyes. In addition, change in IOP after dark-room prone provocative test and change in lens vault from light to dark before LPI were found to be negatively associated with the risk of progression during 14 years after LPI. Based on aforementioned predictors, multivariable logistic models provided good performance in the prediction for long-term risk of progression after LPI (area under the curve = 0.80-0.84). This study suggested that closer monitoring is still required for PACS eyes at high risk of progression even after prophylactic LPI.

INTRODUCTION

Primary angle closure disease (PACD) is a spectrum of diseases characterized by an occludable anterior chamber angle with or without elevated intraocular pressure (IOP) and glaucomatous optic neuropathy (GON).[1] About 24 million people suffer from primary angle closure glaucoma (PACG), the most severe form of PACD, and this number is predicted to increase to 32 million by 2040 due to global aging.[2,3] Laser peripheral iridotomy (LPI) is a safe and effective treatment commonly performed to alleviate pupillary block and widen the angle in all stages of PACD.[4] The landmark Zhongshan Angle Closure Prevention (ZAP) trial[5] and a similar trial in Singapore[6] found that LPI reduced the risk of progression from primary angle closure suspects (PACS) to primary angle closure (PAC) by 45%-47% over 5-6 years.

While most anterior chamber angles widen immediately after LPI treatment, angle widths can regress to baseline or even narrower levels over time, as the result of non pupillary-block mechanisms.[7] Previous studies found that the anterior chamber angle remained closed in 19% to 33% of LPI-treated PACS eyes and 3% could continue to progress after six years despite patent LPI.[4] Compared with the natural history of untreated PACS, progression of angle closure is less common after prophylactic LPI. However, it is still necessary to predict PACS eyes remaining at risk of progression after LPI, which could benefit from closer monitoring.[8] In addition, the prediction can also help to avoid redundant follow-ups for eyes at low risk of progression after LPI.

One primary limitation of the previous 6-year ZAP trial data is that only 19 LPI-treated PACS eyes progressed to PAC – this small number of "positive events" allows for only preliminary analysis for progression and precludes development of robust prediction models based on risk factors before LPI.[9] In this study, we use data from the 14-year ZAP extended follow-up to identify risk factors before LPI for the progression in LPI-treated PACS eyes and develop prediction models for the long-term progression risk after LPI, which can guide post-LPI monitoring and aid personalized angle closure care.

MATERIALS AND METHODS

Study design and population

The design and methodology of ZAP trial (ISRCTN45213099) has been published previously.[10] Screening, enrollment and follow up of ZAP trial participants was conducted in Zhongshan Ophthalmic Center, Guangzhou, China. From 2008 to 2010, a total of 11,991 urban citizens aged 50 to 70 years participated in screening examinations. Patients with bilateral PACS, defined as less than 180° pigmental trabecular meshwork (TM) visible under static gonioscopy, were eligible. Exclusion criteria included presence of peripheral anterior synechiae (PAS), IOP > 21mmHg, GON, history of acute angle closure (AAC), intraocular surgery or trauma, and ocular or systemic diseases that might preclude long-term follow up. Participants with IOP elevation > 15mmHg after the dark-room prone provocative test (DRPPT) were also excluded due to the potential risk of AAC attack. In total, 889 patients met the eligibility criteria and received LPI in one eye selected at random. Performed using the Abraham lens (Ocular Instruments), Yttrium-aluminum-garnet laser (Visulas YAG III; Carl Zeiss Meditec) with a starting energy setting of 1.5 mJ and a minimum diameter of 200-μm spot was focused on the thinnest part of superior iris which could be obscured by the upper lid during eye opening. This study was approved by the Ethical Committee of Zhongshan Ophthalmic Center (2021KYPJ205) and performed in accordance with the tenets of Declaration of Helsinki. Written inform consents were obtained from all participants.

Outcome and follow-up

According to the original protocol, examinations were conducted at baseline, 2 weeks, 0.5, 1.5, 3, 4.5 and 6 years after LPI treatment. All ZAP trial participants were invited to participate in the extended 14-year follow-up based on the same protocol.[11] The primary outcome measured progression to PAC, defined as PAS ≥1 clock hour in any quadrant, IOP > 24 mmHg at two separate visits within one week, or AAC. Eyes receiving cataract surgery before the primary outcome or those lost to follow-up before the 14-year visit were excluded from the current analysis.

Baseline examinations

Ocular structures, including the cornea, anterior chamber, iris, and lens were examined by experienced ophthalmologists using the slit lamp (BQ-900, Haag-Streit). Limbal anterior chamber depth (ACD) was assessed using the modified van Herick grading system, which records anterior chamber depth at limbus as the percentage of peripheral corneal thickness (PCT). The static appearance of anterior chamber angle was evaluated using a Goldmann-type, single-mirror gonioscope (Ocular Instruments) and 1mm narrow light beam under standardized dark room conditions (<1 lux) to avoid light-induced miosis. Care was also taken to avoid excessive indentation or tilting >10° during gonioscopy. Angle width between the peripheral iris and the surface of the trabecular meshwork was scored as 0°, 10°, 20°, 30° or 40° in each quadrant based on the Shaffer grading system. Dynamic gonioscopy was carried out using a Sussman-type, four mirror gonioscope (Ocular Instruments) to identify PAS and differentiate between synechial and appositional angle closure. Gonioscopy examinations were conducted by an experienced ophthalmologist (W.W.) who had good interindividual agreement with examiners in previous follow-ups (weighted kappa >0.80). IOP was measured three times using Goldmann applanation tonometry (Haag-Streit), and the mean value was calculated. In addition, a Tonopen applanation tonometer (TONO-PEN XL, Medtronic) was used to measure IOP before and after DRPPT. During the DRPPT, patients were asked to lie in the dark (<1 lux) with forehead down for 15 minutes. Ultrasound A-scan biometry (CineScan A/B; Quantel Medical) was performed to measure ocular biometric parameters, including axial length (AL), central ACD, and lens thickness (LT).

Anterior-segmental optical coherence tomography (AS-OCT)

AS-OCT (Visante, Carl Zeiss Meditec) scans were performed along the vertical and horizontal meridians of the anterior chamber in the dark (<1 lux). Scans along horizontal meridians were repeated in the light (350-400 lux). Vertical scans were not included in this study due to imaging artifacts associated with the upper and lower eyelids. The semi-automatic analysis of AS-OCT images was performed by a trained grader (C.L.) using the custom software, Zhongshan Angle Assessment Program (ZAAP).[12] Briefly, the scleral spur was manually determined as the point where inner corneal-scleral surface exhibited remarkable alteration in curvature. Then ZAAP automatically outlined borders of cornea and iris, calculated anterior segment parameters (Figure 1), including angle opening distance (AOD_{500}), trabecular-iris space area ($TISA_{500}$) at 500 μm from the scleral spur, angle recess area (ARA_{750}) and iris thickness (IT_{750}) at 750 μm from the scleral spur, iris area (IAREA), iris curvature (ICURV), anterior chamber area (ACA) and width (ACW), lens vault (LV), and pupil diameter (PD). Light-to-dark changes of AS-OCT were calculated by subtracting dark-room metrics from corresponding light-room ones. A set of 80 images (Light-room: Dark-room = 1: 1) from 40 eyes were randomly selected and measured after one month by the grader, with good intraindividual repeatability observed within all parameters (intraclass correlation coefficients: 0.83-1.00).

Statistical analysis

Baseline characteristics were compared between PACS eyes with and without progression using Chi-square tests or Student t-tests. Similar comparisons were performed for eyes included in and excluded from the study. The initial multivariable Logistic models were established based on all independent variables associated with progression from PACS to PAC within 14 years after LPI at the significant level of 0.10, including light-room, and light-to-dark changes of AS-OCT metrics. Adjusted odds ratios (ORs) and 95% confidential intervals (95%CI) were calculated for each variable. A forward stepwise selection method with significance levels for variable entrance and removal of 0.05 and 0.10, respectively, was used to develop final multivariable Logistic models predicting progression. Due to multicollinearity, light-room AOD_{500}, $TISA_{500}$, and ARA_{750} (pairwise correlation coefficients: 0.83, 0.77, 0.88) were included in separate models along with corresponding light-to-dark changes. Sensitivity analyses were performed by replacing AS-OCT parameters measured in the light with those measured in the dark. Nomograms were provided to visualize the predictive value of each variable included in the final models.[13] Discrimination performance was compared using area under receiver operating characteristic curves (AUC) by the DeLong method. Sensitivity, specificity, positive and negative predictive values were reported at cutoff points determined by the Youden index. Decision curves were also generated to assess the clinical utility of prediction models by calculating their net benefits at different threshold probabilities.[14] All statistical analyses were performed on STATA 15.1 (StataCrop). To adjust increased risks of false positive findings, false discovery rates (FDR) were reported in final multivariable models and comparisons of AUC.

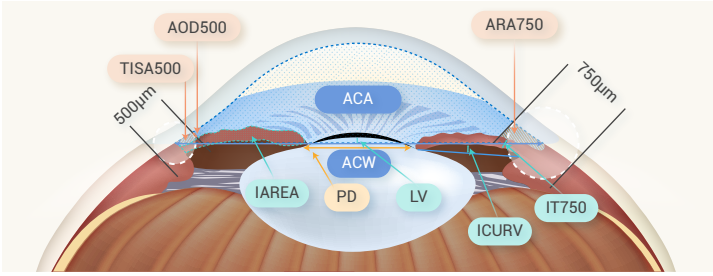

Figure 1. Anterior segment optical coherence tomography metrics determined by the Zhongshan Angle Assessment Program Anterior chamber width (ACW): The horizontal distance between two scleral spurs; Lens vault (LV): The perpendicular distance between the anterior surface of lens and the ACW line; Anterior chamber area (ACA): The cross-sectional area bounded by the posterior surface of corneal endothelium, the anterior surface of lens and iris; Pupil diameter (PD): The shortest distance between two pupil edges; Angle open distance at 500μm (AOD_{500}): The perpendicular distance between the anterior surface of iris and the trabecular meshwork at 500μm from the scleral spur; Trabecular iris space area at 500μm ($TISA_{500}$): The cross-sectional area bounded by the posterior surface of corneal endothelium, the anterior surface of iris, AOD500 and the perpendicular distance between the anterior surface of iris and the scleral spur; Angle recess area at 750μm (ARA_{750}): The cross-sectional area bounded by the posterior surface of corneal endothelium, the anterior surface of iris and the perpendicular distance between the anterior surface of iris and the trabecular meshwork at 750μm from the scleral spur; Iris thickness at 750μm (IT_{750}): The perpendicular distance from the posterior to anterior surface of iris at 750μm from the scleral spur; Iris area (IAREA): the total area of iris from the scleral spur to the pupil; Iris curvature (ICURV): the perpendicular distance from iris pigment epithelium at the point of greatest convexity to the line which connects the most central and peripheral points of iris pigment epithelium.

RESULTS

Among the 889 PACS eyes allocated for LPI intervention, 70 eyes were excluded due to cataract surgery before the primary outcome and 410 eyes were excluded due to loss to the follow-up. Moreover, 39 eyes with undetectable scleral spurs, cornea counters, or iris counters were further excluded from this study. Compared to eligible PACS eyes, excluded eyes had thicker lens and were older on average. The other covariates were comparable between eligible eyes and excluded eyes before LPI (Table S1). In total, 370 eligible eyes (83% from female participants) were included in the current analysis, with an average age of 58.08 ±4.59 years old. During the 14 years of follow-up, 26 eyes progressed from PACS to PAC (7%, 95% CI: 5%-10%), including 22 eyes due to PAS formation and 4 eyes due to elevated IOP. Half of progressed eyes (N = 13) were identified within the first six years after LPI (Table S2) and two eyes were diagnosed with PACG after LPI until the 14-year visit.

Table 1compares baseline parameters between progressed eyes and non-progressed eyes. Compared to eyes without progression, IOP before LPI was higher (16.08 ± 3.33 vs. 14.84 ± 2.77 mmHg, P =0.03) but limbal ACD before LPI was smaller (0.19 ± 0.08 vs. 0.23 ± 0.08 PCT, P =0.02) in PACS eyes with progression during 14 years after LPI. For light-room AS-OCT metrics before LPI, ACA, AOD_{500}, $TISA_{500}$, ARA_{750}, IT_{750}, IAREA and ICURV were smaller but PD was greater in eyes with progression after LPI. For dark-room ones before LPI, ACA, AOD_{500}, $TISA_{500}$, and ARA_{750} were smaller but LV was greater in eyes with progression after LPI. For the changes of AS-OCT metrics from light to dark before LPI, ΔAOD_{500} and ΔIAREA were smaller but ΔPD were greater in progressed eyes (P <0.05). In addition, marginal differences were found in total angle width, ΔIOP after DPRRT, ΔLV, $\Delta TISA_{500}$, and ΔARA_{750} between PACS eyes with and without progression during 14 years after LPI (0.05≤ P <0.10).

In initial model 1 (Table 2), light-room AOD_{500}, light-room ICURV, ΔIOP after DPRRT, and ΔLV were negatively associated with the 14-year risk of progression after LPI in PACS eyes. With light-room AOD_{500} replaced by light-room $TISA_{500}$ and light-room ARA_{750} in initial models 2 and 3, ΔIOP after

Table 1. Comparison of basic measurements and anterior segment optical coherence tomography metrics in PACS eyes before LPI

	Post-LPI progression [a]		Difference (95% CI)	P value
	Yes (n=26)	No (n=344)		
Basic measurements				
Age (years)	59.15 (5.70)	58.00 (4.49)	-1.15 (-2.99 to 0.68)	0.22
Female	22 (85%)	285 (83%)	2% (-12% to 17%)	0.82
Total angle width (score) [b]	4.46 (2.67)	5.39 (2.32)	0.93 (-0.01 to 1.87)	0.05
Limbal ACD (PCT)	0.19 (0.08)	0.23 (0.08)	0.04 (0.01 to 0.07)	0.02
IOP (mmHg)	16.08 (3.33)	14.84 (2.77)	-1.24 (-2.36 to -0.12)	0.03
Δ IOP after DRPPT (mmHg) [c]	3.46 (2.40)	4.50 (2.99)	1.04 (-0.15 to 2.22)	0.09
Axial length (mm)	22.35 (0.84)	22.50 (0.71)	0.16 (-0.13 to 0.45)	0.28
Central ACD (mm)	2.51 (0.23)	2.57 (0.20)	0.06 (-0.02 to 0.14)	0.15
Len thickness (mm)	4.86 (0.25)	4.85 (0.28)	-0.01 (-0.13 to 0.10)	0.82
Light-room AS-OCT metrics				
Light-room ACW (mm)	11.36 (0.42)	11.40 (0.35)	0.05 (-0.10 to 0.19)	0.52
Light-room ACA (mm^2)	14.48 (2.11)	15.28 (1.91)	0.80 (0.03 to 1.56)	0.04
Light-room LV (mm)	0.80 (0.19)	0.75 (0.18)	-0.06 (-0.13 to 0.02)	0.13
Light-room PD (mm)	2.95 (0.74)	2.70 (0.50)	-0.24 (-0.45 to -0.04)	0.02
Light-room AOD_{500} (mm)	0.11 (0.06)	0.16 (0.06)	0.05 (0.03 to 0.07)	<0.01
Light-room $TISA_{500}$ (mm^2)	0.05 (0.02)	0.08 (0.03)	0.03 (0.02 to 0.04)	<0.01
Light-room ARA_{750} (mm^2)	0.11 (0.05)	0.16 (0.06)	0.06 (0.03 to 0.08)	<0.01
Light-room IT_{750} (mm)	0.42 (0.09)	0.46 (0.09)	0.04 (0 to 0.08)	0.03
Light-room IAREA (mm^2)	1.77 (0.31)	1.91 (0.26)	0.14 (0.04 to 0.25)	<0.01
Light-room ICURV (mm)	0.40 (0.08)	0.44 (0.11)	0.04 (0 to 0.09)	0.05
Dark-room AS-OCT metrics				
Dark-room ACW (mm)	11.33 (0.40)	11.39 (0.35)	0.05 (-0.09 to 0.19)	0.45
Dark-room ACA (mm^2)	15.10 (2.05)	15.95 (1.96)	0.85 (0.06 to 1.63)	0.03
Dark-room LV (mm)	0.80 (0.21)	0.73 (0.17)	-0.08 (-0.15 to -0.01)	0.03
Dark-room PD (mm)	4.40 (0.81)	4.42 (0.69)	0.02 (-0.25 to 0.30)	0.86
Dark-room AOD_{500} (mm)	0.06 (0.06)	0.09 (0.05)	0.03 (0.01 to 0.05)	<0.01
Dark-room $TISA_{500}$ (mm^2)	0.03 (0.02)	0.05 (0.03)	0.02 (0.01 to 0.03)	<0.01
Dark-room ARA_{750} (mm^2)	0.07 (0.05)	0.11 (0.05)	0.04 (0.02 to 0.06)	<0.01
Dark-room IT_{750} (mm)	0.48 (0.09)	0.50 (0.09)	0.02 (-0.02 to 0.06)	0.28
Dark-room IAREA (mm^2)	1.52 (0.25)	1.57 (0.21)	0.05 (-0.03 to 0.14)	0.22
Dark-room ICURV (mm)	0.42 (0.08)	0.44 (0.10)	0.01 (-0.03 to 0.05)	0.52
Light-to-dark changes of AS-OCT metrics [d]				
Δ ACW (mm)	0.02 (0.11)	0.01 (0.11)	-0.01 (-0.05 to 0.04)	0.77
Δ ACA (mm^2)	-0.62 (0.32)	-0.67 (0.31)	-0.05 (-0.18 to 0.07)	0.40
Δ LV (mm)	0 (0.06)	0.02 (0.06)	0.02 (0 to 0.05)	0.06
Δ PD (mm)	-1.45 (0.85)	-1.72 (0.64)	-0.27 (-0.53 to -0.01)	0.05
Δ AOD_{500} (mm)	0.05 (0.04)	0.07 (0.05)	0.02 (0 to 0.04)	0.03
Δ $TISA_{500}$ (mm^2)	0.02 (0.02)	0.03 (0.02)	0.01 (0 to 0.01)	0.09
Δ ARA_{750} (mm^2)	0.04 (0.03)	0.06 (0.04)	0.01 (0 to 0.03)	0.08
Δ IT_{750} (mm)	-0.06 (0.05)	-0.04 (0.08)	0.02 (-0.01 to 0.05)	0.23
Δ IAREA (mm^2)	0.25 (0.16)	0.34 (0.17)	0.09 (0.02 to 0.16)	<0.01
Δ ICURV (mm)	-0.03 (0.08)	0 (0.09)	0.03 (-0.01 to 0.07)	0.11

[a] All values were mean (SD) and tested by paired t tests, except the number (%) of females which was tested by chi-square tests; [b] Total angle width was calculated by summing the Shaffer grading of all four quadrants (0-16, with higher scores representing larger angle width); [c] Δ IOP after DRPPT was calculated by subtracting IOP before the test from IOP after the test; [d] Light-to-dark changes of AS-OCT were calculated by subtracting dark-room values from light-room values; PACS=primary angle closure suspect; LPI=laser peripheral iridotomy; 95%CI=95% confidence interval; ACD=Anterior chamber depth; PCT= peripheral corneal thickness; IOP=Intraocular pressure; DRPPT=Dark room prone provocative test; AS-OCT= Anterior segmental optical coherence tomography; ACW=Anterior chamber width; ACA=Anterior chamber area; LV=Lens vault; PD=Pupil diameter; AOD_{500}= Angle opening distance at 500μm; $TISA_{500}$=Trabecular iris space area at 500μm; ARA_{750}= Angle recess area at 750μm; IT_{750}= Iris thickness at 750μm; IAREA= Iris area; ICURV= Iris curvature.

Table 2. Multivariable Logistic regression models for the 14-year risk of progression from PACS to PAC after LPI based on light-room AOD_{500}

Variables	Initial model 1 (Enter)		Final model 1 (Stepwise)	
	OR (95% CI)	P value	OR (95% CI)	FDR
Basic measurements				
Limbal ACD (per 0.01 PCT)	0.94 (0.88 to 1.01)	0.08		
Total angle width (per 1 score increase)	0.90 (0.73 to 1.10)	0.30		
IOP (per 1 mmHg increase)	1.16 (0.98 to 1.37)	0.09		
Δ IOP after DRPPT [a] (per 1 mmHg increase)	0.80 (0.68 to 0.95)	0.01	0.82 (0.70 to 0.97)	0.03
Light-room AS-OCT metrics				
Light-room ACA (per 0.1 mm^2 increase)	0.99 (0.96 to 1.02)	0.38		
Light-room PD (per 0.1 mm increase)	1.08 (0.97 to 1.20)	0.17		
Light-room AOD_{500} (per 0.01 mm increase)	0.83 (0.72 to 0.96)	0.01	0.78 (0.71 to 0.87)	<0.01
Light-room IT_{750} (per 0.1 mm increase)	0.50 (0.22 to 1.13)	0.10	0.58 (0.32 to 1.03)	0.06
Light-room IAREA (per 0.1 mm^2 increase)	0.96 (0.71 to 1.32)	0.82		
Light-room ICURV (per 0.1 mm increase)	0.47 (0.26 to 0.86)	0.01	0.60 (0.36 to 0.97)	0.05
Light-to-dark changes of AS-OCT metrics [b]				
Δ LV (per 0.01 mm increase)	0.89 (0.81 to 0.97)	0.01	0.89 (0.82 to 0.96)	0.02
Δ PD (per 0.1 mm increase)	1.07 (0.96 to 1.20)	0.25		
Δ AOD_{500} (per 0.01 mm increase)	1.00 (0.86 to 1.16)	0.96		
Δ IAREA (per 0.01 mm^2 increase)	1.02 (0.96 to 1.08)	0.54		

[a] Δ IOP after DRPPT was calculated by subtracting IOP before the test from IOP after the test; [b] Light-to-dark changes of AS-OCT were calculated by subtracting dark-room values from light-room values; PACS=Primary angle closure suspect; PAC=Primary angle closure; LPI=Laser peripheral iridotomy; AOD_{500}= Angle opening distance at 500μm; OR=Odds ratio; 95% CI=95% confidence interval; FDR= False discovery rate; ACD= Anterior chamber depth; PCT=Peripheral corneal thickness; IOP=Intraocular pressure; DRPPT: Dark room prone provocative test; ACA=Anterior chamber area; PD=Pupil diameter; IT_{750}= Iris thickness at 750μm; IAREA= Iris area; ICURV= Iris curvature; LV=Lens vault.

Table 3. Multivariable Logistic regression models for the 14-year risk of progression from PACS to PAC after LPI based on light-room $TISA_{500}$

Variables	Initial model 2 (Enter)		Final model 2 (Stepwise)	
	OR (95% CI)	P value	OR (95% CI)	FDR
Basic measurements				
Limbal ACD (per 0.01 PCT)	0.93 (0.87 to 0.99)	0.04		
Total angle width (per 1 score increase)	0.91 (0.74 to 1.12)	0.35		
IOP (per 1 mmHg increase)	1.17 (0.98 to 1.39)	0.09		
Δ IOP after DRPPT [a] (per 1 mmHg increase)	0.81 (0.68 to 0.96)	0.01	0.84 (0.71 to 0.98)	0.03
Light-room AS-OCT metrics				
Light-room ACA (per 0.1 mm^2 increase)	0.98 (0.95 to 1.01)	0.17		
Light-room PD (per 0.1 mm increase)	1.08 (0.97 to 1.21)	0.14		
Light-room $TISA_{500}$ (per 0.01 mm^2 increase)	0.68 (0.52 to 0.88)	<0.01	0.60 (0.49 to 0.74)	<0.01
Light-room IT_{750} (per 0.1 mm increase)	0.68 (0.30 to 1.52)	0.34		
Light-room IAREA (per 0.1 mm^2 increase)	0.95 (0.69 to 1.32)	0.77		
Light-room ICURV (per 0.1 mm increase)	0.59 (0.33 to 1.06)	0.08		
Light-to-dark changes of AS-OCT metrics [b]				
Δ LV (per 0.01 mm increase)	0.89 (0.81 to 0.98)	0.02	0.89 (0.82 to 0.96)	0.01
Δ PD (per 0.1 mm increase)	1.08 (0.97 to 1.20)	0.18		
Δ $TISA_{500}$ (per 0.01 mm^2 increase)	1.11 (0.75 to 1.64)	0.60		
Δ IAREA (per 0.01 mm^2 increase)	1.02 (0.96 to 1.08)	0.58		

[a] Δ IOP after DRPPT was calculated by subtracting IOP before the test from IOP after the test; [b] Light-to-dark changes of AS-OCT were calculated by subtracting dark-room values from light-room values; PACS=Primary angle closure suspect; PAC=Primary angle closure; LPI=Laser peripheral iridotomy; $TISA_{500}$=Trabecular iris space area at 500μm; OR=Odds ratio; 95% CI=95% confidence interval; FDR= False discovery rate; ACD= Anterior chamber depth; PCT=Peripheral corneal thickness; IOP=Intraocular pressure; DRPPT: Dark room prone provocative test; ACA=Anterior chamber area; PD=Pupil diameter; IT_{750}= Iris thickness at 750μm; IAREA= Iris area; ICURV= Iris curvature; LV=Lens vault.

DPRRT and ΔLV remained negatively associated with progression, whereas light-room ICURV did not (Tables 3-4). After forward stepwise selection, final models 1, 2 and 3 included light-room AOD_{500} (OR for 0.01mm increase = 0.78, 95%CI: 0.71-0.87), light-room $TISA_{500}$ (OR for 0.01mm^2 increase = 0.60,

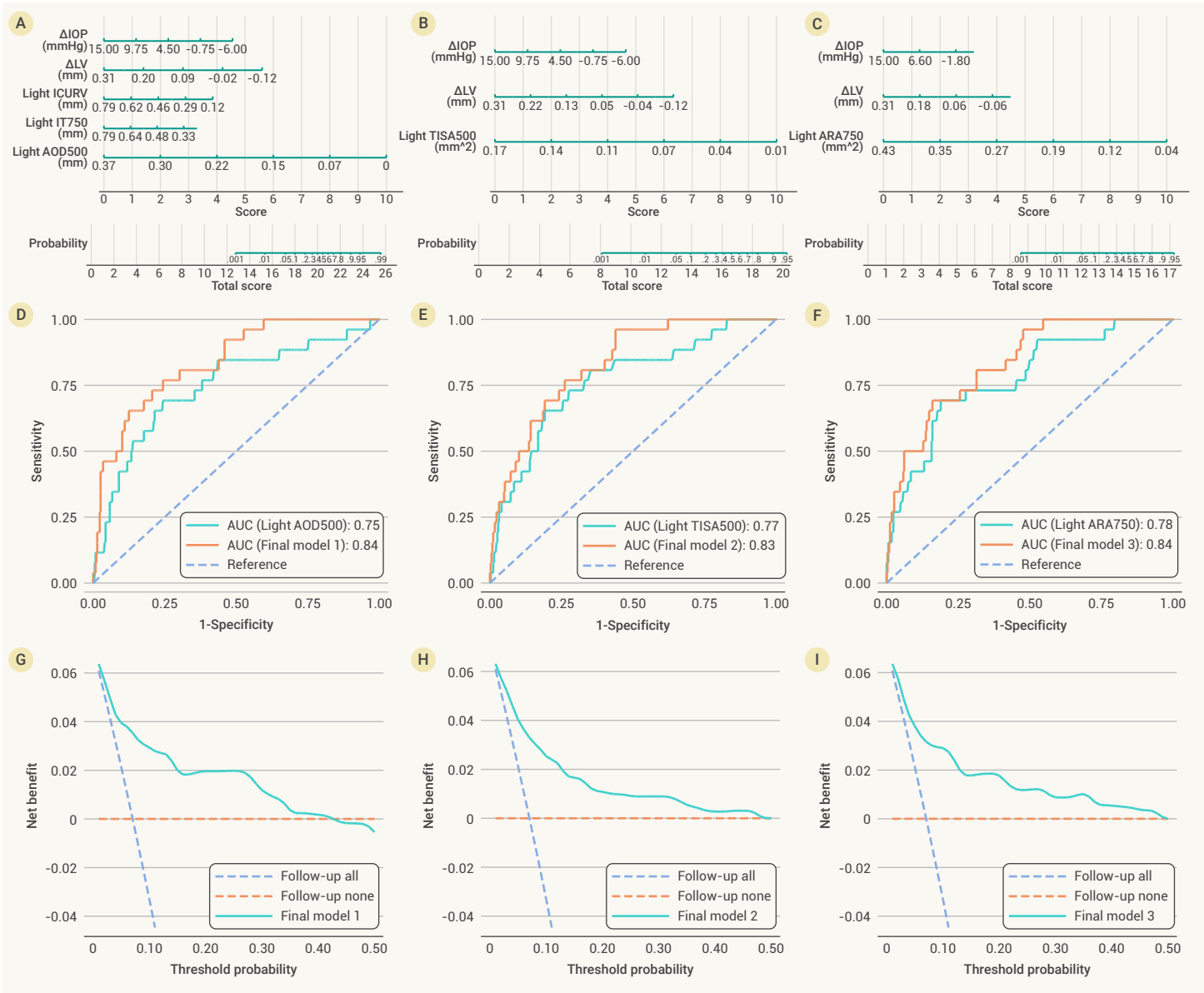

Figure 2. Prediction models for the 14-year risk of progression from PACS to PAC after LPI based on light-room AS-OCT metrics (A-C) By locating examination results on corresponding axes, nomograms assign points for each predictor. The sum points of all predictors determine the 14-year risk of progression from PACS to PAC after LPI; (D-F) Receiver operator characteristics curves summarized predictive performances of risk factors and multivariable models, which are reported as area under the curves; (G-I) Decision curves compare net benefits of prediction for the 14-year risk of progression from PACS to PAC after LPI with hypothetical scenarios that all or none patients received routine follow-up after LPI; Final model 1 included light-room AOD_{500}, light-room IT_{750}, light-room ICURV, Δ LV and Δ IOP after DRPPT; Final model 2 included light-room $TISA_{500}$, Δ LV and Δ IOP after DRPPT; Final model 3 included light-room ARA_{750}, Δ LV and Δ IOP after DRPPT; Δ IOP after DRPPT was calculated by subtracting IOP before the test from IOP after the test; Δ LV was calculated by subtracting the dark-room LV from the light-room LV; PACS=Primary angle closure suspect; PAC=Primary angle closure; LPI=Laser peripheral iridotomy; AS-OCT= Anterior segment optical coherence tomography; AUC= Area under the receiver operating characteristic curve; IOP=Intraocular pressure; DRPPT=Dark room prone provocative test; LV=Lens vault; AOD_{500}= Angle opening distance at 500μm; $TISA_{500}$=Trabecular iris space area at 500μm; ARA_{750}= Angle recess area at 750μm; IT_{750}= Iris thickness at 750μm; ICURV= Iris curvature.

95%CI: 0.49-0.74), and light-room ARA_{750} (OR for 0.01mm^2 increase = 0.75, 95%CI: 0.67-0.84), respectively. The association between ΔLV and the 14-year risk of progression after LPI was consistent (OR for 0.01mm increase = 0.89, 95%CI: 0.82-0.96); however, the association for ΔIOP after DPRRT varied among final models 1, 2, and 3 (OR for per 1 mmHg increase = 0.82-0.84). Final model 1 further included light-room IT_{750} (OR for 0.1mm increase = 0.58, 95%CI: 0.32-1.03) and light-room ICURV (OR for 0.1mm increase = 0.60, 95%CI: 0.36-0.97). With all light-room parameters replaced by dark-room ones, AOD_{500}, $TISA_{500}$, ARA_{750} and corresponding light-to-dark changes were associated with the 14-year risk of progression after LPI, with ΔIOP after DPRRT and ΔLV kept in final models 4, 5, and 6 (Tables S3 & S4). Figures 2 & S1 provide nomograms for predicting the risk of progression from PACS to PAC during the 14 years after LPI in final models 1-6.

Risk factors before LPI including light-room and dark-room AOD_{500}, $TISA_{500}$ and ARA_{750} provided moderate performance (AUC = 0.66-0.78) in prediction for the 14-year risk of progression after LPI (Table 5). Compared with risk factors, multivariable models provided higher predictive efficacy (all FDR <0.05), with AUC = 0.80-0.84 found in final models 1-6 (Figures 2 & S2). At cutoff points determined by the Youden index, final model 2 had the highest sensitivity (0.96, 95%CI= 0.80-1.00) and final model 1 had the highest specificity (0.88, 95%CI= 0.84-0.91), respectively. Risk factors before LPI and multivariable models had high negative predictive values (0.97-0.99) but low positive predictive values at cutoff points. Decision curves (Figures 2 & S3) showed that prediction for the long-term risk of progression in LPI-treated PACS eyes led to net clinical benefits when threshold probabilities < 0.40.

DISCUSSION

Based on 14-year data from the ZAP trial, this study demonstrated that narrowing of anterior chamber angle measured by both light-room and dark-room AS-OCT were significantly associated with the increased risk of

Table 4. Multivariable Logistic regression models for the 14-year risk of progression from PACS to PAC after LPI based on light-room ARA_{750}

Variables	Initial model 3 (Enter)		Final model 3 (Stepwise)	
	OR (95% CI)	P value	OR (95% CI)	FDR
Basic measurements				
Limbal ACD (per 0.01 PCT)	0.93 (0.87 to 1.00)	0.06		
Total angle width (per 1 score increase)	0.92 (0.74 to 1.13)	0.42		
IOP (per 1 mmHg increase)	1.16 (0.97 to 1.38)	0.11		
Δ IOP after DRPPT [a] (per 1 mmHg increase)	0.81 (0.68 to 0.96)	0.02	0.84 (0.72 to 0.99)	0.03
Light-room AS-OCT metrics				
Light-room ACA (per 0.1 mm^2 increase)	0.98 (0.95 to 1.01)	0.28		
Light-room PD (per 0.1 mm increase)	1.07 (0.96 to 1.20)	0.21		
Light-room ARA_{750} (per 0.01 mm^2 increase)	0.79 (0.68 to 0.92)	<0.01	0.75 (0.67 to 0.84)	<0.01
Light-room IT_{750} (per 0.1 mm increase)	0.65 (0.29 to 1.46)	0.30		
Light-room IAREA (per 0.1 mm^2 increase)	0.94 (0.68 to 1.03)	0.72		
Light-room ICURV (per 0.1 mm increase)	0.57 (0.31 to 1.03)	0.06		
Light-to-dark changes of AS-OCT metrics [b]				
Δ LV (per 0.01 mm increase)	0.89 (0.82 to 0.98)	0.02	0.89 (0.82 to 0.96)	0.01
Δ PD (per 0.1 mm increase)	1.09 (0.97 to 1.22)	0.17		
ΔARA_{750} (per 0.01 mm^2 increase)	1.06 (0.85 to 1.32)	0.59		
Δ IAREA (per 0.01 mm^2 increase)	1.02 (0.96 to 1.08)	0.55		

[a] Δ IOP after DRPPT was calculated by subtracting IOP before the test from IOP after the test; [b] Light-to-dark changes of AS-OCT were calculated by subtracting dark-room values from light-room values; PACS=Primary angle closure suspect; PAC=Primary angle closure; LPI=Laser peripheral iridotomy; ARA_{750}= Angle recess area at 750μm; OR=Odds ratio; 95% CI=95% confidence interval; FDR= False discovery rate; ACD= Anterior chamber depth; PCT=Peripheral corneal thickness; IOP=Intraocular pressure; DRPPT: Dark room prone provocative test; ACA=Anterior chamber area; PD=Pupil diameter; IT_{750}= Iris thickness at 750μm; IAREA= Iris area; ICURV= Iris curvature; LV=Lens vault.

Table 5. Performance of risk factors before LPI and multivariable models in the prediction for progression from PACS to PAC during 14 years after LPI

	Sensitivity (95%CI) [a]	Specificity (95%CI) [a]	PPV (95%CI) [a]	NPV (95%CI) [a]	AUC (95%CI)
Risk factors					
Light-room AOD_{500}	0.69 (0.48 to 0.86)	0.76 (0.71 to 0.80)	0.18 (0.11 to 0.26)	0.97 (0.94 to 0.99)	0.75 (0.64 to 0.86)
Light-room $TISA_{500}$	0.65 (0.44 to 0.83)	0.81 (0.76 to 0.85)	0.20 (0.12 to 0.31)	0.97 (0.94 to 0.99)	0.77 (0.67 to 0.87)
Light-room ARA_{750}	0.69 (0.48 to 0.86)	0.81 (0.77 to 0.85)	0.22 (0.13 to 0.32)	0.97 (0.95 to 0.99)	0.78 (0.68 to 0.87)
Dark-room AOD_{500}	0.89 (0.70 to 0.98)	0.42 (0.36 to 0.47)	0.10 (0.07 to 0.15)	0.98 (0.94 to 1.00)	0.66 (0.55 to 0.78)
Dark-room $TISA_{500}$	0.69 (0.48 to 0.86)	0.72 (0.67 to 0.76)	0.16 (0.10 to 0.24)	0.97 (0.94 to 0.99)	0.72 (0.61 to 0.83)
Dark-room ARA_{750}	0.77 (0.56 to 0.91)	0.61 (0.56 to 0.66)	0.13 (0.08 to 0.19)	0.97 (0.94 to 0.99)	0.72 (0.62 to 0.83)
Multivariable models [b]					
Final model 1	0.65 (0.44 to 0.83)	0.88 (0.84 to 0.91)	0.28 (0.17 to 0.41)	0.97 (0.95 to 0.99)	0.84 (0.77 to 0.91)
Final model 2	0.96 (0.80 to 1.00)	0.56 (0.51 to 0.61)	0.14 (0.09 to 0.20)	0.99 (0.97 to 1.00)	0.83 (0.76 to 0.90)
Final model 3	0.69 (0.48 to 0.86)	0.84 (0.80 to 0.88)	0.25 (0.15 to 0.36)	0.97 (0.95 to 0.99)	0.84 (0.76 to 0.91)
Final model 4	0.73 (0.52 to 0.88)	0.73 (0.68 to 0.77)	0.17 (0.10 to 0.25)	0.97 (0.94 to 0.99)	0.80 (0.71 to 0.89)
Final model 5	0.92 (0.75 to 0.99)	0.59 (0.54 to 0.64)	0.15 (0.10 to 0.21)	0.99 (0.97 to 1.00)	0.83 (0.76 to 0.90)
Final model 6	0.69 (0.48 to 0.86)	0.84 (0.80 to 0.88)	0.25 (0.15 to 0.36)	0.97 (0.95 to 0.99)	0.84 (0.76 to 0.91)

[a] Sensitivity, specificity, PPV, and NPV at cutoff values determined by the Youden index and corresponding 95% CIs were presented; [b] Final model 1 included light-room AOD_{500}, light-room IT_{750}, light-room ICURV, Δ LV and Δ IOP after DRPPT. Final model 2 included light-room $TISA_{500}$, Δ LV, and Δ IOP after DRPPT. Final model 3 included light-room ARA_{750}, Δ LV, and Δ IOP after DRPPT. Final model 4 included dark-room AOD_{500}, Δ AOD_{500}, Δ LV, and Δ IOP after DRPPT. Final model 5 included dark-room $TISA_{500}$, Δ $TISA_{500}$, Δ LV, and Δ IOP after DRPPT. Final model 6 included dark-room ARA_{750}, Δ ARA_{750}, Δ LV, and Δ IOP after DRPPT. PACS=Primary angle closure suspect; PAC=Primary angle closure; LPI=Laser peripheral iridotomy; PPV=Positive predictive value; NPV=Negative predictive value; 95%CI=95% confidence interval; IOP=Intraocular pressure; DRPPT: Dark room prone provocative test; LV=Lens vault; AOD_{500}= Angle opening distance at 500μm; $TISA_{500}$=Trabecular iris space area at 500μm; ARA_{750}= Angle recess area at 750μm; IT_{750}= Iris thickness at 750μm; ICURV= Iris curvature.

progression from PACS to PAC within 14 years after LPI. Although angle width and area like AOD_{500}, $TISA_{500}$, and ARA_{750} were promising predictors of the progression in LPI-treated PACS eyes, smaller IOP elevation after DRPPT and LV changes from light to dark were identified as additional risk factors which can improve prediction for the post-LPI progression.

Since LPI alleviates pupillary block through the iris bypass connecting anterior and posterior chambers,[4] progression to PAC after LPI is commonly considered as the result of non pupillary-block mechanisms.[15,16] Plateau iris,

one of most important non pupillary-block factors, is observed in about 30% of residual iridotrabecular contact after LPI.[17] Considering that more than half of angle closure can be attributed to multiple mechanisms,[18] it is hypothesized that PACS eyes that are more severely affected by non pupillary-block factors may benefit less from LPI intervention.

In accordance with previous results, narrow anterior chamber angles before LPI were the most important risk factors for progression from PACS to PAC after LPI.[19] Baskaran et al.[20] found that AOD and ARA at 750 μm from the scleral spur before LPI were smaller in PACS eyes with residual angle closure within the first year after LPI. Another study also suggested that ARA_{750} before LPI was a possible predictor for the alleviation of ITC one month after LPI.[21] Previous 6-year ZAP results supported that both total angle score under static gonioscopy and dark-room $TISA_{500}$ within the first two weeks after LPI were negatively associated with the 6-year risk of progression in LPI-treated PACS eyes.[9] Although some studies reported that LPI-induced angle opening was negatively associated with anterior chamber angle width before LPI, it may only offset partial angle crowdedness (30%-50%). After LPI, some narrow angles can still be crowded and at risk of progression due to non pupillary-block factors.[22,23]

Compared with the dark-room AS-OCT metrics widely used in previous studies, light-room AOD_{500}, $TISA_{500}$, and ARA_{750} provided equivalent or marginally better performance in prediction for the long-term risk of progression from PACS to PAC after LPI. A possible reason is that the iris bombé is relatively flatter when pupil miosis, and the narrowing of anterior chamber angle is more dependent on non pupillary-block mechanisms under light conditions.[24,25] It also explains why the multivariable models based on dark-room angle parameters included corresponding changes from light to dark, which had similar effect sizes as the dark-room metrics.[26]

ΔIOP after DRPPT appeared to be another risk factor for progression in LPI-treated PACS eyes, although its association with the natural history of PACS has been challenged.[27,28] IOP rise after DRPPT is likely influenced by both pupillary dilation and anterior lens movement, so it better reflects dynamic changes in aqueous humor outflow resistance under physiological conditions.[16,29] Compared to anterior chamber angles with similar degrees of crowdedness, those with smaller IOP rise after DRPPT may have weaker pupillary block and more remarkable non pupillary-block factors, which leads to its higher risk of progression after LPI. However, it should be interpreted with caution since there is no evidence to directly verify this hypothesis. Further studies quantifying non pupillary-block factors and testing their associations with IOP changes after DRPPT are warranted to support this finding.

LV, determined by lens thickness and movement, reflects the relative position of lens-iris diaphragm and varies with light-to-dark adaptation. In contrast to the positive association between LV and PAC reported previously by cross-sectional studies,[30,31] the dynamic change of LV from light to dark was negatively associated with the 14-year risk of progression after LPI. Considering that participants excluded due to cataract surgeries or loss to follow-up had greater lens thickness at baseline, the possible influence of selection bias cannot be ruled out which may attenuate the association between static LV and progression after LPI. Different from static LV, dynamic ΔLV offsets the effect of lens thickness and mainly reflects ciliary factors. With anterior direction and rotation of ciliary body,[32] the posterior movement of lens is limited and the crowdedness of the anterior chamber can further lead to angle closure, which contributes to its association with progression from PACS to PAC after the alleviation of pupillary block by LPI.[33]

Our study has several strengths. To our knowledge, this is the largest and longest community-based study on predicting the long-term risk of progression from PACS to PAC after LPI. Different from studying the natural history of PACS, the post-LPI progression reflects residual angle closure secondary to non pupillary-block mechanisms. Compared with previous six-year ZAP data,[9] more progression cases observed in the extended 14 years of follow-up allow the exploration for potential predictors before LPI like dynamic changes of AS-OCT metrics from light to dark and contributes to the better prediction performance. For convenience in practice, the current study also provides nomograms which help to determine PACS eyes at high risk of progression after LPI and guide regular follow-ups.

Our study also has several limitations. First, the Visante AS-OCT suffered from major drawbacks in scan speed and resolution limited by its time-domain scan model.[34] To reduce dropouts due to AS-OCT measurements, this study failed to analyze anterior segmental structures in vertical and oblique B-scans in which the detection of scleral spur was significantly more difficult.[35] With the wide-spread use of swept-source AS-OCT, three-dimensional measurements of anterior chamber angles were expected to improve prediction of progression after LPI in the future. Second, uveal structures originating posterior to the iris, like ciliary body and choroid, were not assessed in this study due to inherent limitations of AS-OCT.[36] Further studies based on ultrasound biomicroscopy are warranted to evaluate non pupillary-block factors such as plateau iris and their association with progression from PACS to PAC after LPI. Third, the rate of PAC progression after LPI was still relatively low compared with previous findings and only two cases of PACG were observed during 14 years.[37] A possible explanation was that previous studies mainly enrolled outpatients but ZAP participants were recruited from community-based screening. It should be noted that about half of LPI-treated eyes were excluded due to cataract surgeries or loss to follow-up, which can also lead to the low rate of progression. Finally, generalizability of current findings to other ethnicities or regions may be limited as ZAP participants were all Chinese living in the urban area.

CONCLUSION

In summary, we found that both light-room and dark-room AS-OCT metrics are promising predictors for the 14-year risk of progression from PACS to PAC after LPI, with higher risk found in eyes with narrower anterior chamber angles, smaller IOP elevation after DRPPT and decreased light-to-dark changes in LV. Prediction models based on these risk factors provide good performance in risk-stratifying for the progression from PACS to PAC after LPI. Despite the protective effect of prophylactic LPI treatment and relatively low risk of PAC occurrence, it may be worthwhile to monitor these high-risk patients more closely to detect further progression.

REFERENCES

1. Prum, B.E., Herndon, L.W., Moroi, S.E., et al. (2016). Primary angle closure preferred practice pattern guidelines. Ophthalmology **123**: P1–P40. DOI: 10.1016/j.ophtha.2015.12.023.
2. Tham, Y.C., Li, X., Wong, T.Y., et al. (2014). Global prevalence of glaucoma and projections of glaucoma burden through 2040: A systematic review and meta-analysis. Ophthalmology **121**: 2081–2090. DOI: 10.1016/j.ophtha.2014.05.013.
3. Quigley, H.A., and Broman, A.T. (2006). The number of people with glaucoma worldwide in 2010 and 2020. Br. J. Ophthalmol. **90**: 262–267. DOI: 10.1136/bjo.2005.081224.
4. Radhakrishnan, S., Chen, P.P., Junk, A.K., et al. (2018). Laser peripheral iridotomy in primary angle closure: A report by the American Academy of Ophthalmology. Ophthalmology **125**: 1110–1120. DOI: 10.1016/j.ophtha.2018.01.015.
5. He, M., Jiang, Y., Huang, S., et al. (2019). Laser peripheral iridotomy for the prevention of angle closure: A single-centre, randomised controlled trial. Lancet **393**: 1609–1618. DOI: 10.1016/S0140-6736(18)32607-2.
6. Baskaran, M., Kumar, R.S., Friedman, D.S., et al. (2022). The Singapore Asymptomatic Narrow Angles Laser Iridotomy Study: Five-year results of a randomized controlled trial. Ophthalmology **129**: 147–158. DOI: 10.1016/j.ophtha.2021.08.017.
7. Jiang, Y., Chang, D.S., Zhu, H., et al. (2014). Longitudinal changes of angle configuration in primary angle-closure suspects: The Zhongshan Angle-Closure Prevention Trial. Ophthalmology **121**: 1699–1705. DOI: 10.1016/j.ophtha.2014.03.039.
8. Yan, W., and He, M. (2017). Predictive medicine in ophthalmology. Ophthalmology **124**: 420–421. DOI: 10.1016/j.ophtha.2016.12.018.
9. Bao, Y.K., Xu, B.Y., Friedman, D.S., et al. (2023). Biometric risk factors for angle closure progression after laser peripheral iridotomy. JAMA Ophthalmol. **141**: 516–524. DOI: 10.1001/jamaophthalmol.2023.0937.
10. Jiang, Y., Friedman, D.S., He, M., et al. (2010). Design and methodology of a randomized controlled trial of laser iridotomy for the prevention of angle closure in southern China: The Zhongshan Angle Closure Prevention Trial. Ophthalmic. Epidemiol. **17**: 321–332. DOI: 10.3109/09286586.2010.508353.
11. Yuan, Y., Wang, W., Xiong, R., et al. (2023). Fourteen-year outcome of angle-closure prevention with laser iridotomy in the Zhongshan Angle-Closure Prevention Study: extended follow-up of a randomized controlled trial. Ophthalmology **130**: 786–794. DOI: 10.1016/j.ophtha.2023.03.024.
12. Console, J.W., Sakata, L.M., Aung, T., et al. (2008). Quantitative analysis of anterior segment optical coherence tomography images: The Zhongshan Angle Assessment Program. Br. J. Ophthalmol. **92**: 1612–1616. DOI: 10.1136/bjo.2007.129932.
13. Kattan, M.W., Eastham, J.A., Stapleton, A.M., et al. (1998). A preoperative nomogram for disease recurrence following radical prostatectomy for prostate cancer. J. Natl. Cancer Inst. **90**: 766–771. DOI: 10.1093/jnci/90.10.766.

14. Vickers, A.J., and Elkin, E.B. (2006). Decision curve analysis: A novel method for evaluating prediction models. Med. Decis. Making **26**: 565–574. DOI: 10.1177/0272989X06295361.
15. Hong, C., Park, K.H., Hyung, S.M., et al. (1996). Evaluation of pupillary block component in angle-closure glaucoma. Jpn. J. Ophthalmol. **40**: 239–243.
16. Sihota, R., Rishi, K., Srinivasan, G., et al. (2016). Functional evaluation of an iridotomy in primary angle closure eyes. Graefes. Arch. Clin. Exp. Ophthalmol. **254**: 1141–1149. DOI: 10.1007/s00417-016-3298-x.
17. Kumar, R.S., Baskaran, M., Chew, P.T., et al. (2008). Prevalence of plateau iris in primary angle closure suspects an ultrasound biomicroscopy study. Ophthalmology **115**: 430–434. DOI: 10.1016/j.ophtha.2007.07.026.
18. Wang, N., Ouyang, J., Zhou, W., et al. (2000). Multiple patterns of angle closure mechanisms in primary angle closure glaucoma in Chinese. Zhonghua Yan Ke Za Zhi **36**: 46–51.
19. Quigley, H.A. (2009). Angle-closure glaucoma-simpler answers to complex mechanisms: LXVI Edward Jackson Memorial Lecture. Am. J. Ophthalmol. **148**: 657–669. DOI: 10.1016/j.ajo.2009.08.009.
20. Baskaran, M., Yang, E., Trikha, S., et al. (2017). Residual angle closure one year after laser peripheral iridotomy in primary angle closure suspects. Am. J. Ophthalmol. **183**: 111–117. DOI: 10.1016/j.ajo.2017.08.016.
21. Koh, V., Keshtkaran, M.R., Hernstadt, D., et al. (2019). Predicting the outcome of laser peripheral iridotomy for primary angle closure suspect eyes using anterior segment optical coherence tomography. Acta Ophthalmol. **97**: e57–e63. DOI: 10.1111/aos.13822.
22. Lee, R.Y., Kasuga, T., Cui, Q.N., et al. (2013). Association between baseline angle width and induced angle opening following prophylactic laser peripheral iridotomy. Invest. Ophthalmol. Vis. Sci. **54**: 3763–3770. DOI: 10.1167/iovs.13-11597.
23. Sung, K.R., Lee, K.S., and Hong, J.W. (2015). Baseline anterior segment parameters associated with the long-term outcome of laser peripheral iridotomy. Curr. Eye Res. **40**: 1128–1133. DOI: 10.3109/02713683.2014.986334.
24. Masoodi, H., Jafarzadehpur, E., Esmaeili, A., et al. (2014). Evaluation of anterior chamber angle under dark and light conditions in angle closure glaucoma: An anterior segment OCT study. Cont. Lens Anterior Eye. **37**: 300–304. DOI: 10.1016/j.clae.2014.04.002.
25. Nolan, W.P., See, J.L., Chew, P.T., et al. (2007). Detection of primary angle closure using anterior segment optical coherence tomography in Asian eyes. Ophthalmology **114**: 33–39. DOI: 10.1016/j.ophtha.2006.05.073.
26. Jiang, Y., Wang, W., Wang, L., et al. (2021). Association of anterior segment parameters and 5-year incident narrow angles: findings from an older Chinese population. Br. J. Ophthalmol. **105**: 970–976. DOI: 10.1136/bjophthalmol-2020-315852.
27. Wilensky, J.T., Kaufman, P.L., Frohlichstein, D, et al. (1993). Follow-up of angle-closure glaucoma suspects. Am. J. Ophthalmol. **115**: 338–346. DOI: 10.1016/S0002-9394(14)73585-8.
28. Friedman, D.S., Chang, D.S., Jiang, Y., et al. (2019). Darkroom prone provocative testing in primary angle closure suspects and those with open angles. Br. J. Ophthalmol. **103**: 1834–1839. DOI: 10.1136/bjophthalmol-2018-313362.
29. Harris, L.S., and Galin, M.A. (1972). Prone provocative testing for narrow angle glaucoma. Arch. Ophthalmol. **87**: 493–496. DOI: 10.1001/archopht.1972.01000020495001.
30. Ozaki, M., Nongpiur, M.E., Aung, T., et al. (2012). Increased lens vault as a risk factor for angle closure: Confirmation in a Japanese population. Graefes. Arch. Clin. Exp. Ophthalmol. **250**: 1863–1868. DOI: 10.1007/s00417-012-2011-y.
31. Moghimi, S., Vahedian, Z., Zandvakil, N., et al. (2014). Role of lens vault in subtypes of angle closure in Iranian subjects. Eye **28**: 337–343. DOI: 10.1038/eye.2013.296.
32. Wang, Z., Chung, C., Lin, J, et al. (2016). Quantitative measurements of the ciliary body in eyes with acute primary-angle closure. Invest. Ophthalmol. Vis. Sci. **57**: 3299–3305. DOI: 10.1167/iovs.16-19558.
33. Tan, G.S., He, M., Zhao, W., et al. (2012). Determinants of lens vault and association with narrow angles in patients from Singapore. Am. J. Ophthalmol. **154**: 39–46. DOI: 10.1016/j.ajo.2012.01.015.
34. Ang, M., Baskaran, M., Werkmeister, R.M., et al. (2018). Anterior segment optical coherence tomography. Prog. Retin. Eye Res. **66**: 132–156. DOI: 10.1016/j.preteyeres.2018.04.002.
35. Sakata, L.M., Lavanya, R., Friedman, D.S., et al. (2008). Assessment of the scleral spur in anterior segment optical coherence tomography images. Arch. Ophthalmol. **126**: 181–185. DOI: 10.1001/archophthalmol.2007.46.
36. Wanichwecharungruang, B., Pattanapongpaiboon, W., Kongsomboon, K., et al. (2022). Diagnostic performance of anterior segment optical coherence tomography in detecting plateau iris. BMJ Open Ophthalmol. **7**: e000931. DOI: 10.1136/bmjophth-2021-000931.
37. Peng, P.H., Nguyen, H., Lin, H.S., et al. (2011). Long-term outcomes of laser iridotomy in Vietnamese patients with primary angle closure. Br. J. Ophthalmol. **95**: 1207–1211. DOI: 10.1136/bjo.2010.181016.

FUNDING AND ACKNOWLEDGMENTS

This study was supported by the Natural Science Foundation of Guangdong Province (grant 2023A1515011475), the Hainan Province Clinical Medical Center, and the Global STEM Professorship Scheme (grant P0046113). Dr. Foster receives additional support from the National Institute for Health Research (NIHR) Biomedical Research Centre at Moorfields Eye Hospital, London, United Kingdom (NIHR-BRC2 009; Moorfields/UCL-IOO), and the Richard Desmond Charitable Foundation. The funders had no role in study design, data collection and analysis, decision to publish or preparation of the manuscript.

AUTHOR CONTRIBUTIONS

Yixiong Yuan: Research execution, data acquisition, data analysis and interpretation, manuscript preparation; Shaopeng Yang: Data acquisition, data analysis and interpretation, manuscript preparation; Wei Wang: Research design, research execution, data acquisition, data analysis and interpretation, manuscript preparation; Benjamin Y. Xu: Data analysis and interpretation, manuscript preparation; Cong Li: Data analysis and interpretation, manuscript preparation; Ruilin Xiong: Research execution, data acquisition, manuscript preparation; Chimei Liao: Research execution, data acquisition; Jian Zhang: Data analysis and interpretation; Qiuxia Yin: Research execution, data acquisition; Yingfeng Zheng: Research execution data acquisition and supervision; David S. Friedman: Research design and supervision; Paul J. Foster: Research design and supervision; Mingguang He: Research design and supervision. The corresponding author has full access to all the data in the study and the final responsibility for the decision to submit for publication.

DECLARATION OF INTERESTS

The authors declare no competing interests.

ETHICAL STATEMENT AND PATIENT CONSENT

This study was approved by the Ethical Committee of Zhongshan Ophthalmic Center (2021KYPJ205) and performed in accordance with the tenets of Declaration of Helsinki. Written inform consents were obtained from all participants.

DATA AND CODE AVAILABILITY

The design and methodology of ZAP trial (ISRCTN45213099) has been published previously. Data are available on reasonable request.

SUPPLEMENTAL INFORMATION

It can be found online at https://doi.org/10.59717/j.xinn-med.2023.100033

LEAD CONTACT WEBSITE

https://orcid.org/0000-0002-5273-3332.